IEEE Access
Multidisciplinary ⋮ Rapid Review ⋮ Open Access Journal

Received April 27, 2022, accepted May 23, 2022, date of publication June 8, 2022, date of current version June 13, 2022.

Digital Object Identifier 10.1109/ACCESS.2022.3180833

Adaptive Neural Task Space Control for Robot Manipulators With Unknown and Closed Control Architecture Under Random Vibrations

CHARLES MEDZO ABA[1], JOSEPH JEAN BAPTISTE MVOGO AHANDA[2], ACHILLE MELINGUI[3], AND ROCHDI MERZOUKI[4]

[1]Department of Physics, Faculty of Sciences, University of Yaoundé 1, Yaoundé, Cameroon
[2]Department of Electrical and Power Engineering, The University of Bamenda, Bamenda, Cameroon
[3]Department of Electrical and Telecommunications Engineering, Ecole Nationale Supérieure Polytechnique, University of Yaoundé 1, Yaoundé, Cameroon
[4]Centre de Recherche en Informatique, Signal et Automatique de Lille Laboratory, UMR, Centre National de la Recherche Scientifique, University of Lille, 59655 Villeneuve d'Ascq, France

Corresponding author: Joseph Jean Baptiste Mvogo Ahanda (josephjeanmvogo@yahoo.fr)

ABSTRACT Robot manipulators are now used in various domains and environments, where they can be subjected to random vibrations. Random vibrations mainly affect the torque control signal, and a torque controller is therefore required to be designed for stabilization purposes. However, for security or intellectual property protection reasons, most commercialized robots are manufactured with unknown and inaccessible torque controller interface such that the user can only design a position/velocity controller. This paper proposes an adaptive task-space velocity controller free from the inner controller's structure and exhibiting stochastic and deterministic disturbances rejection to deal with these issues. To deal with the unknown inner controller, the paper exploits the fact that most torque controllers use a velocity feedback term, and it considers the other terms as an unknown functions vector. To cope with random disturbances, it is demonstrated that the random excitation matrix can be linearly parameterized, and therefore, a direct adaptive method is constructed. Using radial basis function neural network (RBF NN), an indirect adaptive method is developed to cope with deterministic uncertainties. Through Lyapunov theory, the paper proves that all the closed-loop signals are bounded in probability. The effectiveness of the proposed approach is further demonstrated through simulation comparisons.

INDEX TERMS Robot manipulators, adaptive task-space control, closed inner controller, random vibrations, neural networks.

I. INTRODUCTION

The first use of robot manipulators was handling objects in industrial manufacturing lines. In the industrial domain, manipulators evolve in a static and secure environment, where their interactions with this environment are predictable. Nowadays, robot manipulators are used in many domains, such as shipping areas for ship hull maintenance [1], [2], and air transportation for wall painting, fault inspection, or drugs delivery [3], [4]. In most of these usages, it is difficult to stabilize the robot's environment or predict the different interactions between the robot and the environment due to stochastic phenomenons. A robot evolving in a stochastic environment is mainly subject to random vibrations. For example, a robot manipulator used in a boat is subject to boat random movements generated by the waves, whereas an aerial manipulator is exposed to random movements generated by the wind. Therefore, the modeling and control of robot manipulators subject to random vibrations have gained interest for control practitioners, and several solutions have been proposed.

Note that there are two stochastic modeling techniques in the literature, and all existing control schemes use one of these models. The first stochastic modeling approach describes the robot dynamics using Itô-type stochastic differential equations systems (SDEs) and considers random perturbations as white noises. Several control techniques based on an Itô-type stochastic model were proposed in the literature. Cui *et al.* [5] tackled the problem of robot control in a random vibration environment and proposed a vector

The associate editor coordinating the review of this manuscript and approving it for publication was Junhua Li.

form backstepping approach to ensure the convergence of the tracking error mean square to a neighborhood close to zero. The authors in [6] proposed an adaptive dynamic surface control approach to deal with stochastic disturbances. Hui-Fang *et al.* [7] used a neural network-based approximation approach to develop an output feedback control for robot systems subjected to stochastic disturbances. The proposed controller achieves the semi-globally and ultimately uniformly boundedness of the mean square error. Wu *et al.* [8] investigated the issue of tracking control for a benchmark system under random vibrations and developed a vectorial backstepping control approach. Sun *et al.* [9] investigated the tracking control for robot manipulators subjected to state constraints and random disturbances. They achieved system stability through a backstepping controller with a tangent-type constraints term. Sun *et al.* [10] tackle the problem of controlling flexible joint robots subjected to random disturbances from the external environment. They proposed a finite-time adaptive fuzzy command filtered backstepping control approach. Su *et al.* [11] proposed an adaptive neural network controller with unknown control gains for a nonlinear system to achieve stochastic disturbances rejection and ensure full state constraints. The design procedure uses a backstepping technic, and the control gains of the virtual and the main control laws are updated online to achieve the tracking requirements. However, the stochastic Itô-type dynamic model has a drawback related to the fact that it does not represent a natural physical system, and therefore, control approaches based on such a model are difficult to be used in engineering. Indeed, white noise is rarely encountered in a natural environment as it has infinite power. Moreover, some terms in Itô-type modeling, such as Hessian terms, have no physical meaning [12].

To introduce the second stochastic modeling approach, Wu [12] show that an engineering system evolving in a stochastic environment is ideally represented by a system of random differential equations (RDEs) with random perturbations viewed as colored noises and stationary processes. Attractive control schemes using RDEs stochastic model are found in the literature. Cui and Wu [13] developed a vectorial backstepping for the control of flexible joint electrically driven robot manipulators subjected to mechanical and electrical random disturbances. Cui *et al.* [14] investigated the global output feedback tracking control of robot manipulators in random vibrating environments without velocity measurement. However, all these valuable works proposed torque-based controllers, therefore, cannot been used for robot manipulators with inaccessible torque control interface.

Most robot manipulators are manufactured so that the inner controller is designed and embedded by the manufacturer, and the structure is not revealed to the end-user. Indeed, the robot's inner controller structure is not disclosed to the user for security and intellectual property protection reasons, and the torque control interface is not accessible. The user can only design position or velocity commands (outer controller) in this context. Therefore the following problem arises: How to achieve disturbances rejection and high tracking accuracy using only velocity commands? Some research has addressed this issue, and good results have been obtained. For instance, Wang *et al.* [15] developed two adaptive task-space controllers that incorporate a dynamic compensator, where the inner controller is assumed to be a PI (proportional-integral) velocity controller with uncertain design parameters. However, only deterministic disturbances are considered, which means that this solution may yield poor tracking performances for stochastic disturbances. Furthermore, the controller cannot achieve good tracking performances if the actual inner controller is not a PI controller. Khan *et al.* [16] proposed a joint velocity controller which is free from the structure of the inner loop. They deal with the closed structure of the inner controller by considering that a torque controller can be written as a combination of velocity feedback terms and an unknown vector representing the unknown structure. However, this work only consider deterministic uncertainties; therefore, the controller may yield poor tracking performances in a stochastic environment.

One can observe from this brief literature review that there is a need to propose a control strategy for robot manipulators with closed and unknown inner controller working in a random vibrating environment. This paper aims to cope with this problem. Two challenges emerge from this problem, namely: How to deal with the unknown structure and the inaccessibility of the robot's inner controller? How to perform both stochastic and deterministic disturbances rejection? To cope with the first challenge, this paper takes advantage of the fact that for stability purposes, most torque controllers use the velocity feedback term $K_d(\dot{q}-\dot{q}_c)$, with K_d an unknown gain matrix, $\dot{q}$ the joints velocity vector, and $\dot{q}_c$ the joint velocity commands (the outputs of the outer controller). From this observation, it is considered that the inner controller has the form $\tau = -K_d\left(\dot{q}-\dot{q}_c\right)+\Phi\left(q,\dot{q},q_c,\int_0^t q(s)ds,\int_0^t q_c(s)ds\right)$, with Φ an unknown part of the inner controller, whose upper bound is approximated using RBF NN. Therefore, $\dot{q}_c$ is designed such that the unknown vector Φ is canceled in the closed-loop.

For the second challenge, which is performing random disturbances rejection, note that two approaches exist in the literature. In order to present these approaches, let us consider that random excitation dynamics are represented by the matrix $\Gamma(q)\in\mathbb{R}^{n\times r}$, where q is the vector of the n angular positions of the robot joints, and r is the dimension of the task space. The first approach is to separate random disturbances from the robot dynamics and obtain $\|\Gamma(q)\|_F^2$, representing the Frobenius norm of $\Gamma(q)$. In the end, the upper bound (which can be a constant or a linear function) of $\|\Gamma(q)\|_F^2$ is used to perform random vibrations rejection [5], [6], [8], [14]. The second approach separates random disturbances from the robot dynamics to obtain a term dependent on $\Gamma(q)\Gamma^T(q)$; this term is then used to perform random disturbances rejection [13]. However, since $\Gamma(q)$ depends on the robot parameters, these two approaches are sensitive

to modeling errors. Therefore, this paper proposes a direct adaptive random disturbances rejection method to overcome this problem. The proposed adaptive approach is based on the fact that Young's inequality can separate random disturbances from the robot dynamics to obtain the term $\Gamma(q)\Gamma^T(q)y$ with $y \in \mathbb{R}^n$. This term is then used to construct the random disturbances rejection. To design an adaptive approach, this paper demonstrates that the vector $\Gamma(q)\Gamma^T(q)y$ can be linearly parametrizable such that $\Gamma(q)\Gamma^T(q)y = Q(q,y)\Theta$, with $Q(q,y) \in \mathbb{R}^{n\times\bar{m}}$ the regressor, and $\Theta \in \mathbb{R}^{\bar{m}}$ the robot parameters vector. The vector Θ is updated online to improve the accuracy of random disturbances rejection.

Compared with the existing control approaches, the proposed control technique has advantages that are summarized below:

(1) Unlike [5]–[10], this paper considers real practical problems the robot may encounter in various environments. Therefore, the control law developed in this paper has more substantial applicability compared with the previous methods. Furthermore, the proposed control strategy can be used for a robot manipulator with a closed and unknown torque control interface.

(2) Compared with control methods in [13], [14], the proposed adaptive control method is more accurate and less conservative because no assumption is made about the Frobenius norm of random excitation matrix; instead, a direct adaptive method is used. Moreover, the proposed controller has more substantial applicability since it can be applied for robot manipulators with closed or opened torque control interfaces.

(3) In contrast with the control laws in [15], [16], the proposed control technique deals with both deterministic and stochastic uncertainties; therefore, it is adequate for the control of robot manipulators in complex environments. Furthermore, the proposed control approach allows the user to specify the desired tracking performances to improve accuracy.

The rest of this article is organized as follows. In Section II, the preliminaries and problem statement are presented. Section III shows the design procedure. The stability of the closed-loop system is evaluated in Section IV. In Section V, simulations are carried out to verify the effectiveness of the proposed control scheme. Section VI concludes the paper.

Notations: For a vector y, $\|y\|$ stands for its Euclidean norm, y^T denotes its transpose, and $diag(y)$ transforms the vector into a diagonal matrix; For a matrix Y, Y^{-1} is inverse matrix, $\lambda_{\min}(Y)$ and $\lambda_{\max}(Y)$ stands for the minimum and the maximum eigenvalue of Y, respectively; For a scalar α, $\mathbb{E}\alpha$ is its mathematical expectation; $\mathbb{R}^n$ represents the real n-dimensional space; $\mathbb{R}^{n\times r}$ denotes the real $n \times r$ matrix space; $I_{n\times r}$ represents the $n \times r$ unity matrix; $0_{n\times r}$ represents a $n \times r$ matrix with all entries being equal to zero; $1_{n\times r}$ represents a $n \times r$ matrix with all entries being equal to 1. For the sake of simplicity, the function arguments are sometimes omitted.

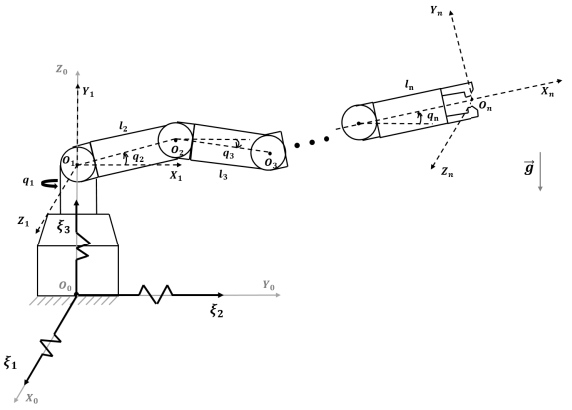

FIGURE 1. *n*-link revolute joints manipulator.

II. PRELIMINARIES AND PROBLEM FORMULATION

A. PROBLEM FORMULATION

Consider an n-DOF revolute joints robot manipulator shown in Fig. 1, with $x \in \mathbb{R}^r$ its end-effector (EE) position in the world frame. The robot is connected to O_0 on the floor and is affected by the environment's random vibrations. Consider that these vibrations result in random accelerations $\xi \in \mathbb{R}^r$ of point O_0. In order to get closer to the real-world context, we consider that these accelerations are stationary and independent processes. With the help of Lagrange's and relative motion theories, the following random model is obtained [13], [14]

$$M(q)\ddot{q} + C(q,\dot{q})\dot{q} + G(q) = \tau + \Gamma(q)\xi, \tag{1}$$

where $\ddot{q} \in \mathbb{R}^n$, $M(q) \in \mathbb{R}^{n\times n}$, $C(q,\dot{q}) \in \mathbb{R}^{n\times n}$, $g(q) \in \mathbb{R}^n$, $\tau \in \mathbb{R}^n$, and $\xi = [\xi_1, \xi_2, \ldots, \xi_r]^T$ are the joint acceleration vector, the inertia matrix, the Coriolis matrix, the gravitational torque, the torque control, and random accelerations vector, respectively. $\Gamma(q) = \left(\Gamma_{ij}(q)\right)_{n\times r}$ is a random excitation matrix. The underlying complete probability space is taken to be a quartet $(\Omega, \mathcal{F}, \mathcal{F}_t, P)$, the filtration $\mathcal{F}_t$ being increasing and right continuous while $\mathcal{F}_0$ contains all P-null sets.

Most commercialized robots have an unknown and inaccessible torque-control interface (inner controller). For security and intellectual property protection purposes, the manufacturer designs the torque controller τ, and the structure is not revealed to the user. The only way to specify joint inputs is through position or velocity commands (outer controller) in such a context. However, when the robot operates in an environment subject to random vibrations, these vibrations affect the actuator torques, as shown in (1). Torque control is the appropriate approach to achieve torque-disturbance rejection, as shown by the many techniques proposed in the literature. However, the user cannot design a torque control law when the robot has a closed and unknown torque-control interface. Therefore, it is tricky to control a robot manipulator with a closed and unknown inner controller and subjected to random vibrations. This paper aims to design

a task-space velocity command $\dot{q}_c$ for the random system (1), which is independent of the embedded torque controller, such that the end-effector trajectory $x(t)$ can track a given bounded reference signal $x_{des}(t)$ (which is assumed at least first-order differentiable) as close as possible while ensuring all the closed-loop signals are bounded in probability.

Before getting into the detailed control scheme, let us summarize the key idea. The general approach for the task-space control is the design of two controllers: a task-space controller (outer controller) $\dot{q}_r = f(q, x, x_{des})$ for the task-space tracking error compensation, and a torque controller (inner controller) $\tau = -K_d(\dot{q} - \dot{q}_r) + g(q, \dot{q}, q_r, \ldots)$ for the joint-space tracking error compensation, with K_d a control gain matrix, $f(q, x, x_{des})$ a smooth function, and $g(q, \dot{q}, q_r, \ldots)$ a smooth function ensuring the gravity or the modeling error compensation, or the stiffness compensation, and so forth [15]. According to the tasks to be executed by the robot, the user can modify f, g, and K_d. However, for robot manipulators with closed-form architecture, τ is already designed by the manufacturer, and the end-user does not know its structure, and he cannot modify it. Furthermore, for the sake of simplicity, the manufacturer does not consider stochastic disturbances during the design of τ. Therefore, for a robot manipulator with closed-form architecture, K_d and $g(q, \dot{q}, q_r, \ldots)$ are unknown, and the random disturbances are not considered. The key idea of the proposed method is the design of a task-space controller $\dot{q}_c = \dot{q}_r - \hat{K}_d^{-1} h(q, \dot{q}, q_r, \ldots)$, where $\hat{K}_d^{-1}$ is the online estimation of K_d^{-1}, and $h(q, \dot{q}, q_r, \ldots)$ is a smooth function ensuring the kinematic and dynamic modeling errors compensation, the rejection of stochastic disturbances, and the compensation of the unknown structure $g(q, \dot{q}, q_r, \ldots)$. Therefore when the inner controller takes $\dot{q}_c$ as input, it is modified as follows: $\tau = -K_d(\dot{q} - \dot{q}_r) - K_d \hat{K}_d^{-1} h(q, \dot{q}, q_r, \ldots) + g(q, \dot{q}, q_r, \ldots)$. The key difficulty of the proposed approach is the design of $\hat{K}_d^{-1}$, and $h(q, \dot{q}, q_r, \ldots)$.

B. RADIAL BASIS FUNCTION NEURAL NETWORK

Nowadays, neural networks (NN) are widely used when approximating uncertain dynamics. The RBF NN is a particular type of NN that uses Gaussian radial basis functions as basis functions. It is well-known that for a continuous function $f(y)$ defined on a compact set $\Im \subset \mathbb{R}^n$, there exists a RBF NN $W_f^T S(y)$ such that for a given positive scalar $\delta_f(y)$ and a positive constant ϵ_f, and a sufficient number of nodes ι, we have [17]

$$f(y) = W_f^T S(y) + \delta_f(y), \tag{2}$$

with $|\delta_f(y)| < \epsilon_f$, and $W_f = [w_1, w_2, \ldots, w_\iota]^T \in \mathbb{R}^\iota$ being the weight vector. Furthermore, $y \in \Im \subset \mathbb{R}^l$ is the input vector and $S(y) = [s_1(y), s_2(y), \ldots, s_\iota(y)]^T$ is the basis function vector, with $s_i(y)$ being a Gaussian function given as

$$s_i(y) = \exp\left[-\frac{(y-\mu_i)^T(y-\mu_i)}{\eta^2}\right], \; i = 1, 2, \ldots, \iota. \tag{3}$$

The vector $\mu_i = [\mu_{i1}, \mu_{i2}, \ldots, \mu_{il}]^T$ is the vector of Gaussian centers, and η the width of Gaussian functions. This paper uses a RBF NN to approximate the upper bound of the robot's nonlinear dynamics.

C. USEFUL PROPERTIES, ASSUMPTIONS AND LEMMAS

The following properties, assumptions, and lemmas are helpful for the ease of controller design.

Proposition 1: The inertia matrix is positive definite, symmetric, and satisfy the following inequality for all $y \in \mathbb{R}^n$ [18]

$$\lambda_{\min}(M(q))||y||^2 \leq y^T M(q) y \leq \lambda_{\max}(M(q))||y||^2. \tag{4}$$

Proposition 2: The inertia and the Coriolis matrix satisfy the following property known as skew symmetry [18]

$$y^T \left(\dot{M}(q) - 2C(q, \dot{q})\right) y = 0, \; \forall y \in \mathbb{R}^n, \tag{5}$$

where $\dot{M}(q)$ is the derivative of the inertia matrix.

Proposition 3: Let $J(q) \in \mathbb{R}^{r \times n}$ be the Jacobian matrix of a n-DOF revolute joint robot manipulator. For any vector $y \in \mathbb{R}^n$, the vector $J(q)y$ is linearly parametrizable in the sense that [16]

$$J(q)y = Y(q, y)\theta, \tag{6}$$

with $Y(q, y) \in \mathbb{R}^{r \times p}$ the kinematic regressor matrix, and $\theta \in \mathbb{R}^p$ the kinematic parameters vector.

Assumption 4: The process $\xi(t)$ is continuous, stationary, and $\mathcal{F}_t$-adapted. There exist a constant $\alpha > 0$ such that for all $t \geq t_0$, [12]

$$\sup_{t_0 \leq s \leq t} \mathbb{E}\|\xi(s)\|^2 \leq \alpha. \tag{7}$$

Lemma 5: For a given n-DOF revolute joint robot manipulator under random vibrations as shown in Fig. 1, the random excitation matrix $\Gamma(q) \in \mathbb{R}^{n \times r}$ is derived such that for all $y \in \mathbb{R}^n$, the vector $\Gamma(q)\Gamma^T(q)y$ is linearly parametrizable in the sense that

$$\Gamma(q)\Gamma^T(q)y = Q(q, y)\Theta, \tag{8}$$

with $\Theta \in \mathbb{R}^{\bar{m}}$ a vector of kinematic and dynamic parameters, and $Q(q, y) \in \mathbb{R}^{n \times \bar{m}}$ a regressor matrix.

The proof of Lemma 5, is given in APPENDIX A.

Lemma 6: Let $S(\bar{b}_l) = \left[S_1(\bar{b}_l), S_2(\bar{b}_l), \ldots, S_\iota(\bar{b}_l)\right]^T$ be a basis function vector of a RBF NN with $\bar{b}_l = [b_1, b_2, \ldots, b_l]^T$. For all k and l chosen such that $0 < k \leq l$, the following inequality holds [17]

$$||S(\bar{b}_l)||^2 \leq ||S(\bar{b}_k)||^2. \tag{9}$$

Lemma 7: For any $y \in \mathbb{R}$ and $\varepsilon > 0$, the following inequality holds [17]

$$0 \leq |y| - y \times \tanh\left(\frac{y}{\varepsilon}\right) \leq 0.2785 \times \varepsilon. \tag{10}$$

Lemma 8: Given two vectors $x, y \in \mathbb{R}^n$ and scalars $a > 0$, $b > 1$ and $c = \frac{b}{b-1}$, the following inequality holds [19]

$$x^T y \leq \frac{a^b}{b}\|x\|^b + \frac{1}{ca^c}\|y\|^c. \tag{11}$$

Remark 9: So far, random excitation dynamics are canceled in the closed-loop system using the upper bound of the norm of the random excitation matrix [5], [14], [20], [21]. In contrast to this approach and for an accurate stochastic disturbances rejection, the method proposed in this paper provides a direct adaptive method using Lemma 5.

III. CONTROL DESIGN

This section presents the task-space velocity controller design procedure. Note that this paper deals with robot manipulators with a closed and unknown inner controller. The latter means that the torque vector τ is designed and already embedded by the manufacturer, but its structure is not revealed to the user and cannot be modified. To overcome this difficulty, we take advantage of the fact that most inner controllers use a velocity feedback term $K_d\left(\dot{q} - \dot{q}_c\right)$ for stability issues [15], [16]. Therefore, we consider that the inner controller has the form

$$\tau = -K_d\left(\dot{q} - \dot{q}_c\right) + \Phi\left(q, \dot{q}, q_c, \int_0^t q(s)ds, \int_0^t q_c(s)ds\right), \tag{12}$$

with $\dot{q}_c$ the joint velocity command (outer controller), K_d the unknown feedback gain matrix, and $\Phi \in \mathbb{R}^{n\times n}$ the unknown part of the inner controller.

Define $\tilde{x} = x(t) - x_{des}(t)$ and $J^{\dagger}(q) = J(q)^T\left[J(q)J(q)^T\right]^{-1}$ the task-space tracking error and the pseudo inverse of the Jacobian matrix $J(q)$, respectively. The computation of the velocity command $\dot{q}_c$ requires the following joint reference velocity

$$\dot{q}_r = \hat{J}^{\dagger}(q)\left[\dot{x}_{des} - \varrho_0\psi(\tilde{x})\right], \tag{13}$$

with $\hat{J}^{\dagger}(q) = \hat{J}(q)^T\left[\hat{J}(q)\hat{J}(q)^T\right]^{-1}$ the estimation of $J^{\dagger}(q)$, $\hat{J}(q)$ the estimation of $J(q)$, and $\varrho_0 = diag(\varrho_{01}, \varrho_{02}, \ldots, \varrho_{0r})$ a positive defined diagonal gain matrix. $\psi(\tilde{x}) \in \mathbb{R}^r$ is a vector defined as

$$\psi(\tilde{x}) = \varrho_1 \times diag\left(\left[\exp\left(\tilde{x}_1^2 - \varpi_1^2\right), .., \exp\left(\tilde{x}_r^2 - \varpi_r^2\right)\right]\right)\tilde{x}, \tag{14}$$

where $\tilde{x}_j$ is the j-th element of $\tilde{x}$, the parameters ϖ_j, $j = 1, 2, \ldots, r$, are the user specified tracking performances, and ϱ_1 a positive design parameter. The parameters ϖ_j represent the maximum task-space tracking errors that the controller can tolerate; therefore, the physical unit of each of them is a mater (m). When the tracking error $\tilde{x}_j$ is out of the expected range $\left[-\varpi_j, \varpi_j\right]$ (that is $\tilde{x}_j^2 > \varpi_j^2$), from the increasing property of the exponential function, the term $\varrho_0\psi(\tilde{x})$ increases to enforce the tracking error's convergence to a neighborhood close to zero. As a result, the convergence rate increases when the tracking performance constraints are violated. In addition, define the joint velocity tracking error as

$$z = \dot{q} - \dot{q}_r. \tag{15}$$

Taking the derivative of (15) and substituting into (1), and using (12), it results in the following joint error dynamic

$$M(q)\dot{z} = -K_d\left(\dot{q} - \dot{q}_c\right) - C(q, \dot{q})z + \Gamma(q)\xi + \Psi(Z), \tag{16}$$

with

$$\Psi(Z) = -\left[M(q)\ddot{q}_r + C(q, \dot{q})\dot{q}_r + G(q) - \Phi\right], \text{ and}$$
$$Z = \left[q, \dot{q}, \dot{q}_r, \ddot{q}_r, q_c, \int_0^t q(s)ds, \int_0^t q_c(s)ds\right]^T. \tag{17}$$

The task-space error dynamic is also required for the controller design. To this end, we use the fact that the task-space velocity $\dot{x}$ and the joint velocity $\dot{q}$ are related as $\dot{x} = J(q)\dot{q}$. Furthermore, from Property 3, one has $J(q)\dot{q} = Y(q, \dot{q})\theta$. Therefore, taking the derivative of $\tilde{x}$ yields to the following task-space error dynamic

$$\begin{aligned}\dot{\tilde{x}} &= \dot{x} - \dot{x}_{des}\\ &= J(q)\dot{q} - \dot{x}_{des}\\ &= Y(q, \dot{q})\tilde{\theta} + Y(q, \dot{q})\hat{\theta} - \dot{x}_{des}\\ &= Y(q, \dot{q})\tilde{\theta} + \hat{J}(q)\dot{q} - \dot{x}_{des}\\ &= -\varrho_0\psi(\tilde{x}) + Y(q, \dot{q})\tilde{\theta} + \hat{J}(q)z,\end{aligned} \tag{18}$$

with $\tilde{\theta} = \theta - \hat{\theta}$, and $\hat{\theta}$ the estimate of the ideal kinematic parameters vector θ.

This paper considers that kinematic and dynamic parameters are uncertain; as a result, the vector $\Psi(Z)$ is uncertain. Therefore, $\Psi(Z)$ represents the deterministic uncertainties while $\Gamma(q)\xi$ represents the stochastic uncertainties. Furthermore, K_d is unknown because the user does not know the structure of the inner controller. The latter means that K_d cannot be taken as a diagonal matrix as it is considered in [15]. Therefore, finding $\dot{q}_c$ which copes with the uncertainties mentioned above while ensuring the stability of the closed-loop system (represented by (16) and (18)) is a challenge. To solve this problem, the following task-space velocity control law is proposed:

$$\dot{q}_c = \dot{q}_r - \hat{\Upsilon}\vartheta, \tag{19}$$

with

$$\vartheta = \hat{\beta}\bar{U} + \hat{J}^T(q)\tilde{x} + \frac{1}{4\varrho_2}Q(q, z)\hat{\Theta}, \tag{20}$$

$\hat{\Upsilon} \in \mathbb{R}^{n\times n}$ the estimation of K_d^{-1}, ϱ_2 a positive design parameter, and $\hat{\beta} \in \mathbb{R}$ the estimation of β the parameter used to build the RBF NN model of the upper bound of $z^T\Psi(Z)$. β is defined as follows

$$\beta = \max\{\delta_{\Psi_1}, \delta_{\Psi_2}, \ldots, \delta_{\Psi_n}, ||W_{\Psi_1}||, \ldots, ||W_{\Psi_n}||\}. \tag{21}$$

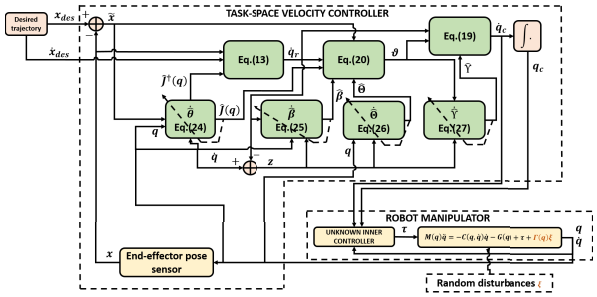

FIGURE 2. Overview of the proposed control scheme.

The vector $\bar{U} \in \mathbb{R}^n$ is chosen as

$$\bar{U} = \left[U_1 \tanh\left(\frac{U_1 z_1}{\varepsilon_1}\right), \ldots, U_n \tanh\left(\frac{U_n z_n}{\varepsilon_n}\right) \right]^T, \quad (22)$$

with $\varepsilon_i > 0$ a design parameter, and z_i the i-th element of z, $i = 1, 2, \ldots, n$. The function U_i is defined as

$$U_i = ||S_i(\bar{Z})|| + 1, \quad (23)$$

with $\bar{Z} = [q, \dot{q}_r]^T$.

The estimation of adaptive parameters θ, β, Θ, and Υ are obtained according to the following laws

$$\dot{\hat{\theta}} = \lambda_1 Y^T(q, \dot{q})\, \tilde{x} - \gamma_1 \hat{\theta}, \quad (24)$$

$$\dot{\hat{\beta}} = \lambda_2 z^T \bar{U} - \gamma_2 \hat{\beta}, \quad (25)$$

$$\dot{\hat{\Theta}} = \frac{\lambda_3}{4\varrho_2} Q^T(q, z)\, z - \gamma_3 \hat{\Theta}, \quad (26)$$

$$\dot{\hat{\Upsilon}}_i = \lambda_{4i} \vartheta_i z - \gamma_{4i} \hat{\Upsilon}_i, \quad (27)$$

where $\hat{\Upsilon}_i$ stands for the i-th column of the matrix $\hat{\Upsilon}$ and ϑ_i the i-th element of ϑ, $i = 1, 2, \ldots, n$. The parameters λ_j, γ_j, λ_{4i}, and γ_{4i}, $j = 1, 2, 3$, are positive design parameters.

For the sake of clarity, Fig. 2 shows the control scheme proposed in this paper.

IV. STABILITY ANALYSIS

In order to evaluate the stability of the controller, let us formulate the following theorem.

Theorem 10: Consider the random model (1) for a n-DOF revolute joint manipulator. Given a bounded reference signal $x_{des}(t)$ being at least first order differentiable, under Assumption 4, the controller (19) with update laws (24), (25), (26), and (27) can ensure that:

(1) The closed-loop system has a unique global solution, and its state has an asymptotic gain in the second moment.
(2) All closed-loop signals are bounded in probability.
(3) The task-space tracking error $\tilde{x}(t) = x(t) - x_{des}(t)$ satisfies

$$\lim_{t\to\infty} \mathbb{E}\|\tilde{x}(t)\|^2 \leq \frac{2(\varrho_2\alpha + \rho_2)}{\rho_3}, \quad (28)$$

where the bound $\frac{2(\varrho_2\alpha+\rho_2)}{\rho_3}$ can become small with an appropriate choice of the design parameters ϖ_k, γ_j, λ_j, ε_i, γ_{4i}, λ_{4i}, ϱ_{0k}, ϱ_1, and ϱ_2, with $i = 1, 2, \ldots, n$, $j = 1, 2, 3$, and $k = 1, 2, \ldots, r$. $\rho_2 = \sum_{i=1}^{n} \frac{\gamma_{4i}}{2\lambda_{4i}} + \rho_1$, and $\rho_1 = \frac{\gamma_1}{\lambda_1}\|\theta\|^2 + \frac{\gamma_2}{\lambda_2}\beta^2 + \frac{\gamma_3}{\lambda_3}\|\Theta\|^2 + 0.2785 \times \beta \sum_{i=1}^{n} \varepsilon_i$. ρ_3 is chosen accordingly to the constraints (60), (61), and (62).

The proof of Theorem 10 is given in APPENDIX B.

Remark 11: It is essential to know how to choose the design parameters to reduce the bound $\frac{2(\varrho_2\alpha+\rho_2)}{\rho_3}$. Note that this bound becomes smaller for ρ_3 taken significant enough, and ϱ_2 and ρ_2 taken small enough. The parameter ρ_2 is small for γ_j and γ_{4i} chosen as mall as possible, and λ_j and λ_{4i} chosen significant enough, $j = 1, 2, 3$, $i = 1, 2, \ldots, n$. From the latter, it is tricky to find a significant value for ρ_3 that fulfills the constraints (60), (61), and (62). Furthermore, tacking a small value for ϱ_2 can result in a large control signal as shown in (20). Therefore, a trade-off must be found between the tracking performance requirements and the fulfillment of constraints through the trial and error method.

V. SIMULATION RESULTS

To demonstrate the effectiveness of the proposed control scheme, we carry out simulations tests using a 5-DOF revolute joint robot manipulator with kinematic, dynamic, and Denavit-Hartenberg (DH) parameters given in Tab. 1. d_1 and d_5 are the link 1 and link 5 offset, α_1 and α_4 are the link 1 and link 4 twist, and l_i is the link length, $i = 1, 2, 3, 4$. In this study, two groups of simulation studies are carried out. The first group aims to study the effect of the main design parameters ϖ_j and ϱ_2 on the tracking performances, $j = 1, 2, 3$. The second group aims to show the superiority of the proposed controller over the observer-based adaptive control developed in [15]. For the two groups of simulation tests, the desired EE trajectory is given as

$$x_{des} = \Big[0.2 + 0.1\cos\Big(\frac{\pi}{12.5}t\Big), 0.2 + 0.1\sin\Big(\frac{\pi}{12.5}t\Big), 0.4 + 0.2\sin\Big(\frac{\pi}{12.5}t\Big)\Big]^T. \quad (29)$$

The 5-DOF revolute joint robot using in this study has the joint position defined as: q_1, the base rotation angle, q_2, the shoulder rotation angle, q_3, the elbow rotation angle, q_4, the wrist pitch angle, and q_5, the wrist roll angle. For the Cartesian trajectory tracking, the wrist roll angle q_5 remains unchanged (that is $q_5(t) = q_5(0) = 0rad$). Therefore, the control signal for this axis will be zero, $\dot{q}_{c5}(t) = 0rad/s$.

Throughout the study its assumed that the robot's inner controller is a PI velocity controller given as

$$\tau = -K_d(\dot{q} - \dot{q}_c) - K_i(q - q_c), \quad (30)$$

with $K_d = K_i = diag(10 \times \mathbf{1}_{5\times 1})$.

Decomposing ξ_1, ξ_2, and ξ_3 in each link's frame as indicated in [5], and using the explicit formula for the random

TABLE 1. Kinematic and dynamic parameters for the 5-DOF robot.

Link number	DH parameters to SI [a]	link mass [kg]
1	$d_1 = 0.35\text{m}, l_1 = 0.016\text{m},$ $\alpha_1 = \pi/2$ rad, $I_{xx} = 0.8 \times 10^{-3}\text{kg.m}^2,$ $I_{yy} = 1.6 \times 10^{-3}\text{kg.m}^2$ $I_{zz} = 1.9 \times 10^{-3}\text{kg.m}^2,$ $I_{xy} = 0.6 \times 10^{-3}\text{kg.m}^2$	2
2	$l_2 = 0.22\text{m},$ $I_{xx} = 799.9 \times 10^{-6}\text{kg.m}^2,$ $I_{yy} = 1.7 \times 10^{-3}\text{kg.m}^2,$ $I_{zz} = 1.7 \times 10^{-3}\text{kg.m}^2$	3
3	$l_3 = 0.22\text{m},$ $I_{xx} = 0.8 \times 10^{-3}\text{kg.m}^2,$ $I_{yy} = 12.5 \times 10^{-3}\text{kg.m}^2,$ $I_{zz} = 12.5 \times 10^{-3}\text{kg.m}^2$	3
4	$l_4 = 0\text{m}, \alpha_4 = \pi/2$ rad, $I_{xx} = 0.6 \times 10^{-3}\text{kg.m}^2,$ $I_{yy} = 0.6 \times 10^{-3}\text{kg.m}^2,$ $I_{zz} = 0.3 \times 10^{-3}\text{kg.m}^2$	1.7
5	$d_5 = 0.15\text{m},$ $I_{xx} = 0.9 \times 10^{-3}\text{kg.m}^2,$ $I_{yy} = 0.9 \times 10^{-3}\text{kg.m}^2,$ $I_{zz} = 0.2 \times 10^{-3}\text{kg.m}^2$	0.8

[a] m = meter; kg = kilogram; rad = radian.

excitation matrix (39), it follows that

$$
\begin{aligned}
&\Gamma_{11}(q)\\
&\quad = -m_1 l_{c1}\sin(q_1) + m_1 l_1 \sin(q_1)\\
&\qquad + m_4 l_3 \cos(q_1)\cos(q_2)^2\cos(q_3)^2\sin(q_4)\\
&\qquad - m_4 l_3 \cos(q_1)\cos(q_2)\cos(q_3)\sin(q_4)\sin(q2)\sin(q_3)\\
&\qquad + m_4 l_2 \cos(q_1)\cos(q_2)^2\cos(q_3)\sin(q_4)\\
&\qquad + m_4 l_1 \cos(q_1)\cos(q_2)\cos(q_3)\sin(q_4)\\
&\Gamma_{12}(q)\\
&\quad = m_1 l_{c1}\cos(q_1) - m_1 l_1 \cos(q_1)\\
&\qquad + m_4 l_3 \sin(q_1)\cos(q_2)^2\cos(q_3)^2\sin(q_4)\\
&\qquad - m_4 l_3 \cos(q_2)\cos(q_3)\sin(q_4)\sin(q_2)\sin(q_3)\sin(q_1)\\
&\qquad + m_4 l_2 \sin(q_1)\cos(q_2)^2\cos(q_3)\sin(q_4)\\
&\qquad + m_4 l_1 \cos(q_2)\cos(q_3)\sin(q_4)\sin(q_1)\\
&\Gamma_{13}(q)\\
&\quad = m_4\sin(q_4)\sin(q_2)\cos(q_3)\left(l_3\cos(q_2)\cos(q_3)\right.\\
&\qquad \left. - l_3\sin(q_2)\sin(q_3) + l_2\cos(q_2) + l_1\right), \qquad (31)\\
&\Gamma_{21}(q)\\
&\quad = -\cos(q_1)\left(-m_3 l_{c3}\cos(q_2)\sin(q_3)\right.\\
&\qquad + m_3 l_3\cos(q_2)\sin(q_3) + m_3 l_2\sin(q_3)\cos(q_3)\cos(q_2)\\
&\qquad \left. + m_2 l_{c2}\sin(q_2) - m_2 l_2\sin(q_2)\right)\\
&\Gamma_{22}(q)\\
&\quad = -\sin(q_1)\left(-m_3 l_{c3}\cos(q_2)\sin(q_3)\right.\\
&\qquad + m_3 l_3\cos(q_2)\sin(q_3) + m_3 l_2\sin(q_3)\cos(q_3)\cos(q_2)\\
&\qquad \left. + m_2 l_{c2}\sin(q_2) - m_2 l_2\sin(q_2)\right)\\
&\Gamma_{23}(q)\\
&\quad = -m_2\cos(q_2)l_2 + m_2 l_{c2}\cos(q_2)\\
&\qquad + m_3 l_{c3}\sin(q_2)\sin(q_3) - m_3 l_3\sin(q_2)\sin(q_3)\\
&\qquad - m_3 l_2\sin(q_3)\cos(q_3)\sin(q_2)\\
&\Gamma_{31}(q)\\
&\quad = -m_3\left(l_3 - l_{c3}\right)\cos(q_1)\cos(q_2)\sin(q_3)\\
&\Gamma_{32}(q)\\
&\quad = -m_3\left(l_3 - l_{c3}\right)\sin(q_1)\cos(q_2)\sin(q_3)\\
&\Gamma_{33}(q)\\
&\quad = -m_3\left(l_3 - l_{c3}\right)\sin(q_2)\sin(q_3), \qquad (32)
\end{aligned}
$$

with $\Gamma_{i1} = \Gamma_{i2} = \Gamma_{i3} = 0$, for $i = 4, 5$. From (31), (32) and (40), the regressor $Q(q, z) \in \mathbb{R}^{5\times 28}$, and the vector of kinematic and dynamic parameters $\Theta \in \mathbb{R}^{28}$ can be easily computed. The random vibrations ξ_1, ξ_2 and ξ_3 are produced as follows [5]

$$
b_i\dot{\xi}_i(t) = -\xi_i(t) + w_i(t),\ \xi_i(0) = 0,\ i = 1, 2, 3, \qquad (33)
$$

with $b_i > 0$, and $w_i(t)$ a zero-mean band limited white noise with a power A_i and a sample time t_c. The means square value of the zero mean stationary process ξ_i is given as $\mathbb{E}\|\xi_i(t)\|^2 = \frac{A_i}{\pi b_i}\arctan\left(\frac{\pi b_i}{50t_c}\right)$. For this simulation study, we choose $b_i = 0.5$, $t_c = 0.05$, and $A_i = 2$, which result in $\mathbb{E}\|\xi_i(t)\|^2 = 0.7143$.

1) COMPARATIVE SIMULATIONS WITH DIFFERENT DESIGN PARAMETERS

Among the design parameters that can improve the tracking performances, ϖ_j and ϱ_2 are the most important. Indeed, ϖ_j can improve the transient performances of the closed-loop system, whereas ϱ_2 can ameliorate the steady-state performances as stated in Remark 11. This section carries out simulations tests using different ϖ_j and ϱ_2 values to verify these properties. During these tests, the other design parameters are chosen as: $\varepsilon_i = 5$, $\lambda_2 = 10$, $\gamma_1 = \gamma_2 = \gamma_3 = \gamma_{4_i} = 0.01$, $\varrho_0 = diag(\mathbf{1}_{3\times 1})$, $\varrho_1 = 1$, and $\lambda_1 = \lambda_{4_i} = 3$, $i = 1, 2, \ldots, 5$. Initial values are taken as: $q(0) = [0.6,\ 0.4,\ 0.2,\ 0,\ 0]^T$, $\dot{q}(0) = \mathbf{0}_{5\times 1}$, $\hat{\beta}(0) = 0.04$, $\hat{\theta}(0) = 0.5 \times \mathbf{1}_{4\times 1}$, $\Theta(0) = 0.4 \times \mathbf{1}_{28\times 1}$, and $\hat{\Upsilon}(0) = diag(10 \times \mathbf{1}_{5\times 1})$.

For the first group of simulation tests, we choose $\varpi_j = 0.001$, $j = 1, 2, 3$, whereas three different values for ϱ_2 are used, that is $\varrho_2 = \{0.01,\ 0.5,\ 1\}$. Simulations results are given in Fig. 3 and Fig. 4. Fig. 3 depicts the EE trajectory tracking errors for different values of ϱ_2. It is observed that during the transient phase (that is $t \leq 2Sec$), the lowest settling time is obtained for $\varrho_2 = 1$, the highest settling time is obtained for $\varrho_2 = 0.01$, and the highest bound for the tracking error (that is $|\tilde{x}_j(t)| \leq 0.103m$) is obtained for $\varrho_2 = 1$. At the steady-state phase, it is observed that $|\tilde{x}_j(t)| \leq 2 \times 10^{-3}m$ for $\varrho_2 = 1$, and $|\tilde{x}_j(t)| \leq 2 \times 10^{-4}m$ for $\varrho_2 = 0.01$. From Fig. 4, it is observed that at the transient phase, the highest bound of the control signals (that is $|\dot{q}_{ci}(t)| \leq 1.1\ rad/s$) is obtained for $\varrho_2 = 0.01$, whereas for $\varrho_2 = 1$, the

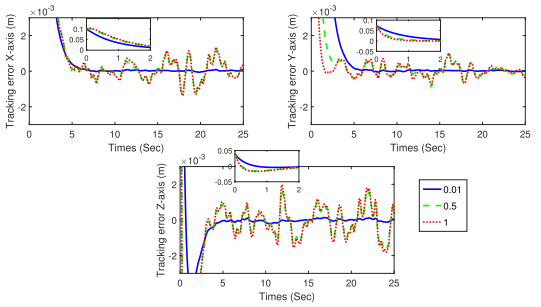

FIGURE 3. Simulation results for $\varrho_2 = \{0.01,\ 0.5,\ 1\}$: Tracking errors in X-axis, Y-axis, and Z-axis.

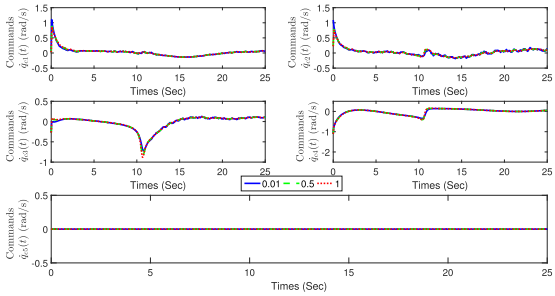

FIGURE 4. Simulation results for $\varrho_2 = \{0.01,\ 0.5,\ 1\}$: Velocity commands $\dot{q}_{ci}$, $i = 1, 2, \ldots, 5$.

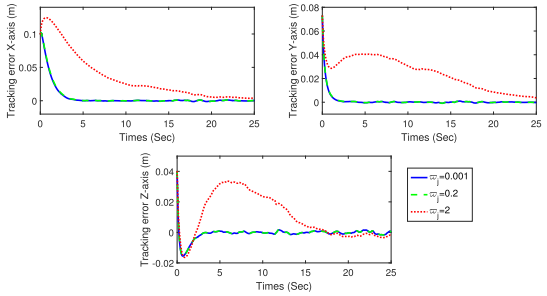

FIGURE 5. Simulation results for $\varpi_j = \{0.001,\ 0.2,\ 2\}$, $j = 1, 2, 3$: Tracking errors in X-axis, Y-axis, and Z-axis.

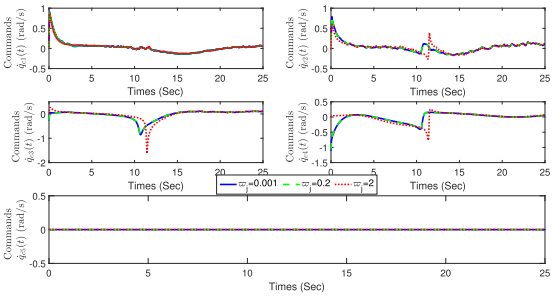

FIGURE 6. Simulation results for $\varpi_j = \{0.001,\ 0.2,\ 2\}$, $j = 1, 2, 3$: Velocity commands $\dot{q}_{ci}$, $i = 1, 2, \ldots, 5$.

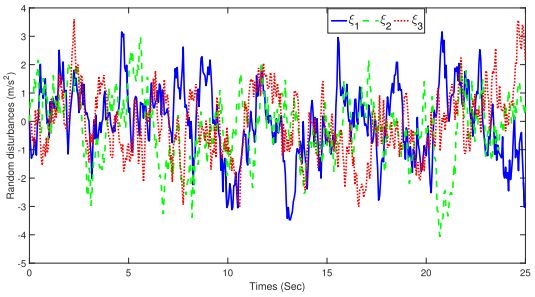

FIGURE 7. Random accelerations ξ_1, ξ_2, and ξ_3 of the robot's connection point to ground.

bound is 0.86 rad/s. These observations show that the lowest the parameter ϱ_2 is, the better are the tracking performances, but with a high control demand at the transient stage. These results are compatible with expectations because from (28) a low value for ϱ_2 results in a low value for $\mathbb{E}\left\|\tilde{x}\left(t\right)\right\|^2$, whereas from (20) a low value of ϱ_2 can lead to high control demands. Therefore, ϱ_2 must be chosen according to the admissible maximum actuator velocity.

For the last group of simulation tests, we choose $\varrho_2 = 0.5$, whereas three different values for ϖ_j are used, that is, $\varpi_j = \{10^{-3},\ 0.2,\ 2\}$. Fig. 5 and Fig. 6 give the simulation results. From Fig. 5, it is observed that the lowest tracking error (that is $\left|\tilde{x}_j\left(t\right)\right| \leq 1.2 \times 10^{-3} m$) is obtained for $\varpi_j = 0.001$. From Fig. 6, the control signals are higher for $\varpi_j = 2$ at the steady-state, but the highest control signal is observed for $\varpi_j = 0.001$ at the transient phase. These results show that a low value for ϖ_j leads to good steady-state and transient performances and high control demand at the transient phase. These results confirm the effectiveness of the disturbances rejection due to $\psi\left(\tilde{x}\right)$. Indeed, when the constraint $\tilde{x}_j^2 \leq \varpi_j^2$ is not fulfilled (mainly encountered at the transient phase), $\psi\left(\tilde{x}\right)$ increases the control gain $\varrho_1\varrho_{0j}$ to improve the disturbances rejection. However, ϖ_j must be chosen according to the admissible maximum actuator velocity.

2) COMPARATIVE SIMULATIONS WITH THE OBSERVER-BASED ADAPTIVE TRACKING CONTROL SCHEME DEVELOPED IN [15]

This section aims to prove the superiority of the proposed control scheme over the controller developed in [15]. The design parameters for the proposed controller are chosen as $\varpi_j = 0.001$, $j = 1, 2, 3$, and $\varrho_2 = 0.01$. For the controller in [15] the design parameters are taken as: $\gamma = diag\left([5, 5, 10]\right)$, $\Gamma_d = I_{54}$, $\Lambda = 0.01 I_5$, $\Lambda_I = 0.2 I_5$, $\hat{a}_d(0) = 0_{54}$, and $\hat{w}_I(0) = 2 \times \mathbf{1}_{5\times 1}$.

The simulation results are given in Figs. 7, 8, and 9. Fig. 7 depicts the random accelerations chosen for this study. Note that these random accelerations are the worst-case encountered in the real world. Fig. 8 presents the EE trajectory and the EE trajectory tracking errors for the two controllers. It is observed that the two controllers achieve the EE trajectory tracking. The proposed controller performs the lowest settling time at the transient phase ($t \leq 4Sec$). At the steady-state phase, tracking error is bounded as $\left|\tilde{x}_j\left(t\right)\right| \leq 1.5 \times 10^{-4} m$ for the proposed controller, and as $\left|\tilde{x}_j\left(t\right)\right| \leq 2 \times 10^{-3} m$ for the controller in [15]. Control

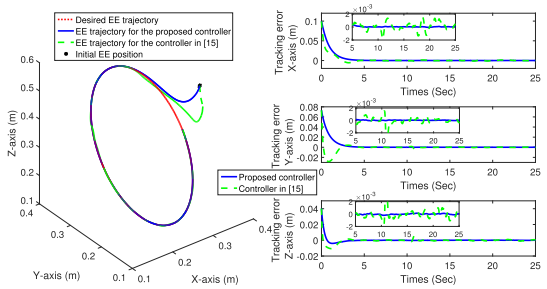

FIGURE 8. Comparative simulation results: EE trajectory and tracking errors for the two controllers.

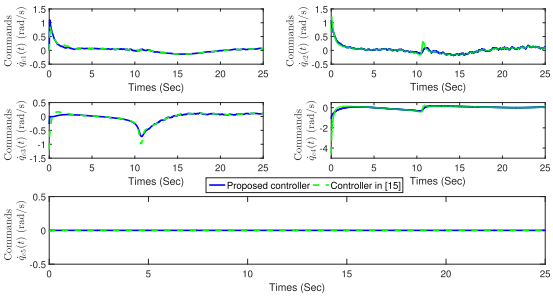

FIGURE 9. Comparative simulation results: Velocity commands $\dot{q}_{ci}$, $i = 1, 2, \ldots, 5$ for the two controllers.

demands for the two controllers are given in Fig. 9. It is observed that $|\dot{q}_{ci}(t)| \leq 1.1\ rad/s$ for the proposed controller, and $|\dot{q}_{ci}(t)| \leq 5\ rad/s$ for the controller in [15]. Therefore, the proposed controller performs the best tracking performances with low control signals. Two reasons can explain these observations. The first reason is that in contrast to the observer-based adaptive tracking control scheme [15] our controller exhibits both deterministic and stochastic disturbances rejection. The second reason is that, for the proposed controller, $\psi(\tilde{x})$ allows the designer to impose the required tracking performances. Note that, in contrast to the method in [15], the proposed controller is free from the structure of the inner controller; consequently it can be used for any robot manipulator.

At the end of these simulation studies, it appears that, in contrast to the literature, the proposed control approach presents better tracking performances, with the lowest control signals. These good performances can be explained by the ability of the controller to achieve both deterministic and stochastic disturbances rejection. Moreover, through the $\psi(\tilde{x})$ vector and particularly the ϖ_j parameters, the controller succeeds in maintaining the constraint $\tilde{x}_j(t)^2 \leq \varpi_j^2$, which improves the tracking accuracy even in the presence of significant disturbances. Note that the designer does not need to know the robot's inner controller structure to implement the proposed controller.

VI. CONCLUSION

This paper considers the problem of tracking control of a robot manipulator with a closed and unknown inner controller under random vibrations. A direct adaptive method is proposed to achieve a stochastic disturbances rejection. An indirect RBF NN adaptive method is used to deal with deterministic uncertainties. Based on the fact that most inner controllers use a velocity feedback term, an adaptive velocity controller is designed to be free from the structure of the inner controller. Through Lyapunov theory, the paper shows that the tracking error is bounded in probability. Simulation comparisons demonstrate the effectiveness of the proposed control strategy.

APPENDIX A
PROOF OF LEMMA 1

Before proceeding to the proof of the Lemma 5, let us recall the modeling procedure of the effect of random vibrations on a planar robot manipulator, developed by Cui *et al.* [5]. Indeed, they consider that due to the random vibrations of the robot's environment, the robot's connection point to the ground O_0 acquires an acceleration $\xi \in \mathbb{R}^r$. This acceleration propagates along the robot arms and generates in each arm's center of mass, a stochastic inertial force ${}^iF_{ci} = -m_i {}^ia_{ci2}$, where m_i is the i-th link mass, and ${}^ia_{ci2}$ the projection of ξ in the Y-direction (if the link evolve in the vertical plane) or in the Z-direction (if the link evolve in the horizontal plane) of the i-th link frame. Therefore, the stochastic torque $\tau_c = \Gamma(q)\,\xi$ is the generalized stochastic inertial force.

Now let us find the explicit formula for the random excitation matrix $\Gamma(q)$ for any revolute joint robot manipulator. For this purpose, define $\check{x}_{ci} = \left[{}^ix_{ci}^T,\ 1\right]^T$ and $\check{F}_{ci} = \left[{}^iF_{ci}^T,\ 0\right]^T$, where ${}^ix_{ci} \in \mathbb{R}^r$ is the position of the i-th link center of mass in the i-th link frame. Define ${}^0H_i \in \mathbb{R}^{(r+1)\times(r+1)}$, the homogeneous transformation describing the relative position between the base frame and the i-th link frame. The generalized stochastic force along the j-th generalized coordinates is given as [5]

$$\tau_{cj} = \sum_{i=1}^{n}\sum_{s=1}^{r}\left(F_{ci}(s)\,\frac{\partial x_{ci}(s)}{\partial q_j}\right), \tag{34}$$

where $F_{ci}(s)$ and $x_{ci}(s)$ are the s-th element of F_{ci} and x_{ci}, respectively. F_{ci} and x_{ci} are the stochastic inertial force, and the position of i-th link center for mass in the base frame, respectively. Using the homogeneous transformation ${}^0H_i$, (34) can be rewritten as

$$\begin{aligned}\tau_{cj} &= \sum_{i=1}^{n}\left({}^0H_i\check{F}_{ci}\right)^T\left(\frac{\partial}{\partial q_j}{}^0H_i\check{x}_{ci}\right)\\ &= \sum_{i=1}^{n}\check{F}_{ci}^T{}^0H_i^T\left(\frac{\partial}{\partial q_j}{}^0H_i\right)\check{x}_{ci}.\end{aligned} \tag{35}$$

From the definition of ${}^ia_{ci2}$, there exist a matrix $\Omega_i(q) \in \mathbb{R}^{(r+1)\times(r+1)}$ such that

$$\check{F}_{ci} = m_i\Omega_i(q)\,\check{\xi}, \tag{36}$$

with $\check{\xi} = \left[\xi^T,\ 1\right]^T$.

Note that for a revolute joint robot one has $\frac{\partial}{\partial q_j}{}^0H_i = 0_{(r+1)\times(r+1)}$, for $j > i$. Using the latter and (36) in (35) it follows

$$\begin{aligned}\tau_{cj} &= \sum_{i=j}^{n} m_i \check{\xi}^T \Omega_i^T {}^0H_i^T \left(\frac{\partial}{\partial q_j}{}^0H_i\right) \check{x}_{ci} \\ &= \sum_{i=j}^{n} \left(m_i \check{x}_{ci}^T \left(\frac{\partial}{\partial q_j}{}^0H_i\right)^T {}^0H_i \Omega_i\right) \check{\xi} \\ &= \left[\Gamma_{j\times r},\ 1\right] \check{\xi}, \end{aligned} \tag{37}$$

with

$$\left[\Gamma_{j\times r},\ 1\right] = \sum_{i=j}^{n} \left(m_i \check{x}_{ci}^T \left(\frac{\partial}{\partial q_j}{}^0H_i\right)^T {}^0H_i \Omega_i\right), \tag{38}$$

and $\Gamma_{j\times r}$ the j-line of $\Gamma(q)$.

From (38) it follows the explicit formula for the elements of $\Gamma(q)$ as

$$\Gamma_{js} = \sum_{i=j}^{n} m_i \check{x}_{ci}^T \left[\left(\frac{\partial}{\partial q_j}{}^0H_i\right)^T {}^0H_i \Omega_i\right]_{(r+1)\times s}, \tag{39}$$

with $1 \le j \le n$, and $1 \le s \le r$. It is known that for a revolute joint robot, ${}^0H_i$ depends linearly on kinematic parameters. Therefore, from (39), we can conclude that Γ_{js} depends linearly on dynamic and kinematic parameters.

Now define $v, y \in \mathbb{R}^n$ such that $v = \Gamma(q)\Gamma^T(q)y$. The j-th element of v is given as

$$v_j = \sum_{s=1}^{n}\sum_{k=1}^{r} \Gamma_{jk}\Gamma_{sk} y_s, \tag{40}$$

with y_s the s-th element of y. Since Γ_{js} depends linearly on dynamic and kinematic parameters, from (40) we can easily conclude that v_j depends linearly on kinematic and dynamic parameters. The latter means that v can be linearly parameterizable. In order words, we can found a matrix $Q(q,y) \in \mathbb{R}^{n\times\bar{m}}$ and a vector of robot's dynamic and kinematic parameters $\Theta \in \mathbb{R}^{\bar{m}}$ such that $\Gamma(q)\Gamma^T(q)y = Q(q,y)\Theta$, this ends the proof □

APPENDIX B
PROOF OF THEOREM 1

The closed-loop signals are $z, \tilde{x}, \tilde{\theta} = \theta - \hat{\theta}, \tilde{\beta} = \beta - \hat{\beta}, \tilde{\Theta} = \Theta - \hat{\Theta}$, and $\tilde{\Upsilon}_i$ the i-th column of the matrix $\tilde{\Upsilon} = K_d^{-1} - \hat{\Upsilon}$. Therefore, we can define the Lyapunov candidate $V(t) \in \mathbb{R}$ of the closed-loop system as follows

$$\begin{aligned} V(t) = {} & \frac{1}{2}z^T M(q) z + \frac{1}{2}\tilde{x}^T\tilde{x} + \frac{1}{2\lambda_1}\tilde{\theta}^T\tilde{\theta} + \frac{1}{2\lambda_2}\tilde{\beta}^2 \\ & + \frac{1}{2\lambda_3}\tilde{\Theta}^T\tilde{\Theta} + \frac{1}{2}\sum_{i=1}^{n}\frac{1}{\lambda_{4i}}\tilde{\Upsilon}_i^T K_d \tilde{\Upsilon}_i. \end{aligned} \tag{41}$$

Taking the derivative of (41), using (16), (18), and Property 2, it follows

$$\begin{aligned} \dot{V}(t) = {} & \frac{1}{2}z^T\left[\dot{M}(q) - 2C(q,\dot{q})\right] - z^T K_d(\dot{q} - \dot{q}_c) z \\ & + z^T\Gamma(q)\xi + z^T\Psi(Z) + \tilde{x}^T\dot{\tilde{x}} + \frac{1}{\lambda_1}\tilde{\theta}^T\dot{\tilde{\theta}} \\ & + \frac{1}{\lambda_2}\tilde{\beta}\dot{\tilde{\beta}} + \frac{1}{\lambda_3}\tilde{\Theta}^T\dot{\tilde{\Theta}} + \sum_{i=1}^{n}\frac{1}{\lambda_{4i}}\tilde{\Upsilon}_i^T K_d \dot{\tilde{\Upsilon}}_i \\ = {} & -z^T K_d(\dot{q} - \dot{q}_c) z + z^T\Gamma(q)\xi + z^T\Psi(Z) \\ & - \varrho_0\tilde{x}^T\psi(\tilde{x}) + \tilde{x}^T Y(q,\dot{q})\tilde{\theta} + \tilde{x}^T\hat{J}(q) z \\ & + \frac{1}{\lambda_1}\tilde{\theta}^T\dot{\tilde{\theta}} + \frac{1}{\lambda_2}\tilde{\beta}\dot{\tilde{\beta}} + \frac{1}{\lambda_3}\tilde{\Theta}^T\dot{\tilde{\Theta}} \\ & + \sum_{i=1}^{n}\frac{1}{\lambda_{4i}}\tilde{\Upsilon}_i^T K_d \dot{\tilde{\Upsilon}}_i. \end{aligned} \tag{42}$$

The parameter β, the parameters vectors θ and Θ, and K_{di}^{-1} the i-th column of K_d^{-1} are constants. Therefore, the following equalities hold

$$\dot{\tilde{\beta}} = -\dot{\hat{\beta}}; \quad \dot{\tilde{\theta}} = -\dot{\hat{\theta}}; \quad \dot{\tilde{\Theta}} = -\dot{\hat{\Theta}}; \quad \dot{\tilde{\Upsilon}}_i = -\dot{\hat{\Upsilon}}_i. \tag{43}$$

From Lemma 5 and Lemma 8, the following inequalities hold

$$\begin{aligned} z^T\Gamma(q)\xi &\le \frac{1}{4\varrho_2} z^T\Gamma(q)\Gamma^T(q) z + \varrho_2\|\xi\|^2 \\ &\le \frac{1}{4\varrho_2} z^T Q(q,z)\Theta + \varrho_2\|\xi\|^2. \end{aligned} \tag{44}$$

The vector $\Psi(Z)$ is unknown; therefore, from (2), its components $\Psi_i(Z)$ can be approximated with a RBF NN model as follows

$$\Psi_i(Z) = W_{\Psi_i}^T S_i(Z) + \delta_{\Psi_i}(Z), \tag{45}$$

with $|\delta_{\Psi_i}(Z)| \le \epsilon_{\Psi_i}$, $i = 1, 2, \ldots, n$. From (21), (22), (23), (45), Lemmas 6 and 7, the nonlinear function $z^T\Psi(Z)$ is bounded as follows

$$\begin{aligned} z^T\Psi(Z) &= \sum_{i=1}^{n} z_i\left[W_{\Psi_i}^T S_i(Z) + \delta_{\Psi_i}(Z)\right] \\ &\le \sum_{i=1}^{n}|z_i|\left[\|W_{\Psi_i}^T\|\|S_i(Z)\| + |\delta_{\Psi_i}(Z)|\right] \\ &\le \beta\sum_{i=1}^{n}|z_i|\left[\|S_i(Z)\| + 1\right] \\ &\le \beta\sum_{i=1}^{n}|z_i|\left[\|S_i(\bar{Z})\| + 1\right] \\ &\le \beta\sum_{i=1}^{n}|z_i U_i| \\ &\le \beta z^T\bar{U} + 0.2785\times\beta\sum_{i=1}^{n}\varepsilon_i. \end{aligned} \tag{46}$$

Using (19), (43), (44), and (46) into (42), yields

$$\begin{aligned} \dot{V}(t) \le {} & -z^T K_d(\dot{q} - \dot{q}_c) + \frac{1}{4\varrho_2} z^T Q(q,z)\Theta \\ & + \varrho_2\|\xi\|^2 + \beta z^T\bar{U} + 0.2785\times\beta\sum_{i=1}^{n}\varepsilon_i \\ & - \varrho_0\tilde{x}^T\psi(\tilde{x}) + \tilde{x}^T Y(q,\dot{q})\tilde{\theta} + \tilde{x}^T\hat{J}(q) z \\ & - \frac{1}{\lambda_1}\tilde{\theta}^T\dot{\hat{\theta}} - \frac{1}{\lambda_2}\tilde{\beta}\dot{\hat{\beta}} - \frac{1}{\lambda_3}\tilde{\Theta}^T\dot{\hat{\Theta}} \end{aligned}$$

$$
\begin{aligned}
&-\sum_{i=1}^{n}\frac{1}{\lambda_{4i}}\tilde{\Upsilon}_i^T K_d\dot{\hat{\Upsilon}}_i\\
&\leq -z^T K_d z-\varrho_0\tilde{x}^T\psi\left(\tilde{x}\right)-z^T K_d\hat{\Upsilon}\vartheta\\
&\quad+\frac{1}{4\varrho_2}z^T Q\left(q,z\right)\Theta+\varrho_2\|\xi\|^2+\beta z^T\bar{U}\\
&\quad+0.2785\times\beta\sum_{i=1}^{n}\varepsilon_i+\tilde{\theta}^T Y\left(q,\dot{q}\right)\tilde{x}\\
&\quad+z^T\hat{J}\left(q\right)\tilde{x}-\frac{1}{\lambda_1}\tilde{\theta}^T\dot{\hat{\theta}}-\frac{1}{\lambda_2}\tilde{\beta}\dot{\hat{\beta}}\\
&\quad-\frac{1}{\lambda_3}\tilde{\Theta}^T\dot{\hat{\Theta}}-\sum_{i=1}^{n}\frac{1}{\lambda_{4i}}\tilde{\Upsilon}_i^T K_d\dot{\hat{\Upsilon}}_i\\
&\leq -z^T K_d z-\varrho_0\tilde{x}^T\psi\left(\tilde{x}\right)-z^T K_d\hat{\Upsilon}\vartheta\\
&\quad+\varrho_2\|\xi\|^2+0.2785\times\beta\sum_{i=1}^{n}\varepsilon_i\\
&\quad+z^T\left[\hat{\beta}\bar{U}+\hat{J}\left(q\right)\tilde{x}+\frac{1}{4\varrho_2}Q\left(q,z\right)\hat{\Theta}\right]\\
&\quad+\frac{1}{\lambda_1}\tilde{\theta}^T\left[\lambda_1 Y\left(q,\dot{q}\right)\tilde{x}-\dot{\hat{\theta}}\right]\\
&\quad+\frac{1}{\lambda_2}\tilde{\beta}\left[\lambda_2 z^T\bar{U}-\dot{\hat{\beta}}\right]-\sum_{i=1}^{n}\frac{1}{\lambda_{4i}}\tilde{\Upsilon}_i^T K_d\dot{\hat{\Upsilon}}_i\\
&\quad+\frac{1}{\lambda_3}\tilde{\Theta}^T\left[\frac{\lambda_3}{4\varrho_2}Q\left(q,z\right)z-\dot{\hat{\Theta}}\right].
\end{aligned}
\tag{47}
$$

Substituting (20), (24), (25), and (26) into (47) one has

$$
\begin{aligned}
\dot{V}\left(t\right)\leq\ &-z^T K_d z-\varrho_0\tilde{x}^T\psi\left(\tilde{x}\right)+\varrho_2\|\xi\|^2\\
&+z^T\left[\mathbf{1}_{n\times n}-K_d\hat{\Upsilon}\right]\vartheta+\frac{\gamma_1}{\lambda_1}\tilde{\theta}^T\hat{\theta}\\
&+\frac{\gamma_2}{\lambda_2}\tilde{\beta}\hat{\beta}+\frac{\gamma_3}{\lambda_3}\tilde{\Theta}^T\hat{\Theta}-\sum_{i=1}^{n}\frac{1}{\lambda_{4i}}\tilde{\Upsilon}_i^T K_d\dot{\hat{\Upsilon}}_i\\
&+0.2785\times\beta\sum_{i=1}^{n}\varepsilon_i.
\end{aligned}
\tag{48}
$$

Note that the following inequalities hold

$$
\begin{aligned}
\frac{\gamma_1}{\lambda_1}\tilde{\theta}^T\hat{\theta}&\leq-\frac{\gamma_1}{\lambda_1}\tilde{\theta}^T\tilde{\theta}+\frac{\gamma_1}{\lambda_1}\|\theta\|^2\\
\frac{\gamma_2}{\lambda_2}\tilde{\beta}\hat{\beta}&\leq-\frac{\gamma_2}{\lambda_2}\tilde{\beta}^2+\frac{\gamma_2}{\lambda_2}\beta^2\\
\frac{\gamma_3}{\lambda_3}\tilde{\theta}^T\hat{\theta}&\leq-\frac{\gamma_3}{\lambda_3}\tilde{\Theta}^T\tilde{\Theta}+\frac{\gamma_3}{\lambda_3}\|\Theta\|^2.
\end{aligned}
\tag{49}
$$

Substituting (49) into (48) and using the fact that $\mathbf{1}_{n\times n}-K_d\hat{\Upsilon}=K_d\tilde{\Upsilon}$, it follows that

$$
\begin{aligned}
\dot{V}\left(t\right)\leq\ &-z^T K_d z-\varrho_0\tilde{x}^T\psi\left(\tilde{x}\right)-\frac{\gamma_1}{\lambda_1}\tilde{\theta}^T\tilde{\theta}\\
&-\frac{\gamma_2}{\lambda_2}\tilde{\beta}^2-\frac{\gamma_3}{\lambda_3}\tilde{\Theta}^T\tilde{\Theta}+z^T K_d\tilde{\Upsilon}\vartheta\\
&-\sum_{i=1}^{n}\frac{1}{\lambda_{4i}}\tilde{\Upsilon}_i^T K_d\dot{\hat{\Upsilon}}_i+\varrho_2\|\xi\|^2+\rho_1,
\end{aligned}
\tag{50}
$$

with $\rho_1=\frac{\gamma_1}{\lambda_1}\|\theta\|^2+\frac{\gamma_2}{\lambda_2}\beta^2+\frac{\gamma_3}{\lambda_3}\|\Theta\|^2+0.2785\times\beta\sum_{i=1}^{n}\varepsilon_i$.

Since $\tilde{\Upsilon}$ is a matrix and z a vector, the term $z^T K_d\tilde{\Upsilon}\vartheta$ can be rewritten as

$$
z^T K_d\tilde{\Upsilon}\vartheta=\sum_{i=1}^{n}\tilde{\Upsilon}_i^T\vartheta_i K_d z,
\tag{51}
$$

with ϑ_i the i-th element of ϑ, $i=1,2,\ldots,n$.

Substituting (27) and (51) into (50) yields

$$
\begin{aligned}
\dot{V}\left(t\right)&\leq-z^T K_d z-\varrho_0\tilde{x}^T\psi\left(\tilde{x}\right)-\frac{\gamma_1}{\lambda_1}\tilde{\theta}^T\tilde{\theta}-\frac{\gamma_2}{\lambda_2}\tilde{\beta}^2\\
&\quad-\frac{\gamma_3}{\lambda_3}\tilde{\Theta}^T\tilde{\Theta}+\sum_{i=1}^{n}\frac{1}{\lambda_{4i}}\tilde{\Upsilon}_i^T K_d\left[\lambda_{4i}\vartheta_i z-\dot{\hat{\Upsilon}}_i\right],\\
&\quad+\varrho_2\|\xi\|^2+\rho_1\\
&\leq-z^T K_d z-\varrho_0\tilde{x}^T\psi\left(\tilde{x}\right)-\frac{\gamma_1}{\lambda_1}\tilde{\theta}^T\tilde{\theta}-\frac{\gamma_2}{\lambda_2}\tilde{\beta}^2\\
&\quad-\frac{\gamma_3}{\lambda_3}\tilde{\Theta}^T\tilde{\Theta}-\sum_{i=1}^{n}\frac{\gamma_{4i}}{\lambda_{4i}}\tilde{\Upsilon}_i^T K_d\tilde{\Upsilon}_i\\
&\quad+\sum_{i=1}^{n}\frac{\gamma_{4i}}{\lambda_{4i}}\tilde{\Upsilon}_i^T K_d K_{di}^{-1}+\varrho_2\|\xi\|^2+\rho_1.
\end{aligned}
\tag{52}
$$

Note that $K_d K_{di}^{-1}$ is a vector with the i-th element equal to 1, whereas all the other elements are zero. Therefore, the following equality holds

$$
\left(K_d K_{di}^{-1}\right)^T\left(K_d K_{di}^{-1}\right)=1,\ \forall\, i=1,2,\ldots,n.
\tag{53}
$$

From (53) and Lemma 8 it follows

$$
\sum_{i=1}^{n}\frac{\gamma_{4i}}{\lambda_{4i}}\tilde{\Upsilon}_i^T K_d K_{di}^{-1}\leq\sum_{i=1}^{n}\frac{\gamma_{4i}}{2\lambda_{4i}}\tilde{\Upsilon}_i^T\tilde{\Upsilon}_i+\sum_{i=1}^{n}\frac{\gamma_{4i}}{2\lambda_{4i}}.
\tag{54}
$$

Substituting (54) into (52) results in

$$
\begin{aligned}
\dot{V}\left(t\right)&\leq-z^T K_d z-\varrho_0\tilde{x}^T\psi\left(\tilde{x}\right)-\frac{\gamma_1}{\lambda_1}\tilde{\theta}^T\tilde{\theta}-\frac{\gamma_2}{\lambda_2}\tilde{\beta}^2\\
&\quad-\frac{\gamma_3}{\lambda_3}\tilde{\Theta}^T\tilde{\Theta}-\sum_{i=1}^{n}\frac{\gamma_{4i}}{\lambda_{4i}}\tilde{\Upsilon}_i^T\left(K_d-\frac{1}{2}I_{n\times n}\right)\tilde{\Upsilon}_i\\
&\quad+\varrho_2\|\xi\|^2+\rho_2,
\end{aligned}
\tag{55}
$$

with $\rho_2=\sum_{i=1}^{n}\frac{\gamma_{4i}}{2\lambda_{4i}}+\rho_1$.

In this study, K_d is assumed to be unknown for the user. Therefore, the sign of $K_d-\frac{1}{2}I_{n\times n}$ is not known a priori. Nevertheless, we should notice that the feedback gains K_{dii} are chosen significantly enough to reduce the settling time and the tracking error for most torque controllers. Therefore, for most practical cases, $K_{dii}\gg\frac{1}{2}$ such that the matrices K_d and $K_d-\frac{1}{2}I_{n\times n}$ are positive definite [22], [23]. The latter means that for all $y\in\mathbb{R}^n$, the following inequalities hold:

$$
0\leq\lambda_{\min}\left(K_d\right)y^T y\leq y^T K_d y\leq\lambda_{\max}\left(K_d\right)y^T y
\tag{56}
$$

$$
0\leq y^T\left(K_d-\frac{1}{2}I_{n\times n}\right)y.
\tag{57}
$$

From the increasing property of the function $\exp\left(x\right)$, it follows

$$
\begin{aligned}
-\varrho_0\tilde{x}^T\psi\left(\tilde{x}\right)\leq-\tilde{x}^T diag\Big(\Big[&\varrho_{01}\varrho_1\exp\left(-\varpi_1^2\right),\\
&\ldots,\varrho_{0r}\varrho_1\exp\left(-\varpi_r^2\right)\Big]\Big)\tilde{x}.
\end{aligned}
\tag{58}
$$

Using (56), (57) and (58) into (55), it follows

$$\begin{aligned}\dot{V}(t) \leq & -\lambda_{\min}(K_d) z^T z - \frac{\gamma_1}{\lambda_1}\tilde{\theta}^T\tilde{\theta} - \frac{\gamma_2}{\lambda_2}\tilde{\beta}^2 + \varrho_2\|\xi\|^2 \\ & -\frac{\gamma_3}{\lambda_3}\tilde{\Theta}^T\tilde{\Theta} - \sum_{i=1}^{n}\frac{\gamma_{4i}}{\lambda_{4i}}\tilde{\Upsilon}_i^T\left(K_d - \frac{1}{2}I_{n\times n}\right)\tilde{\Upsilon}_i \\ & +\rho_2 - \tilde{x}^T diag\left(\left[\varrho_{01}\varrho_1\exp\left(-\varpi_1^2\right),\right.\right. \\ & \left.\left.\ldots,\varrho_{0r}\varrho_1\exp\left(-\varpi_r^2\right)\right]\right)\tilde{x}. \end{aligned} \tag{59}$$

From (56) and (57), and the fact that inertia matrix $M(q)$ is positive definite, for all $y \in \mathbb{R}^n$, there exist a positive constant ρ_3 that fulfills the following three constraints

$$\rho_3 \leq \min\left\{2\varrho_{0j}\varrho_1\exp\left(-\varpi_j^2\right), 2\gamma_k\right\}, \tag{60}$$

$$\frac{\rho_3}{2}\lambda_{\max}(M(y)) \leq \lambda_{\min}(K_d), \tag{61}$$

and

$$\frac{\rho_3}{2}y^T K_d y \leq \gamma_{4i} y^T\left(K_d - \frac{1}{2}I_{n\times n}\right)y, \tag{62}$$

with $k = 1, 2, 3, j = 1, 2, \ldots, r$, and $i = 1, 2, \ldots, n$.

Using (41), (60), (61), (62), and Property 1 into (59) it follows

$$\begin{aligned}\dot{V}(t) \leq & -\frac{\rho_3}{2}z^T M(q) z - \frac{\rho_3}{2\lambda_1}\tilde{\theta}^T\tilde{\theta} - \frac{\rho_3}{2\lambda_2}\tilde{\beta}^2 \\ & -\frac{\rho_3}{2\lambda_3}\tilde{\Theta}^T\tilde{\Theta} - \sum_{i=1}^{n}\frac{\rho_3}{2\lambda_{4i}}\tilde{\Upsilon}_i^T K_d\tilde{\Upsilon}_i \\ & -\frac{\rho_3}{2}\tilde{x}^T\tilde{x} + \varrho_2\|\xi\|^2 + \rho_2 \\ \leq & -\rho_3 V(t) + \varrho_2\|\xi\|^2 + \rho_2. \end{aligned} \tag{63}$$

Taking expectations on both sides of (63) and using Assumption 4, one has

$$\begin{aligned}\mathbb{E}\dot{V}(t) \leq & -\rho_3\mathbb{E}V(t) + \varrho_2\mathbb{E}\|\xi\|^2 + \rho_2 \\ \leq & -\rho_3\mathbb{E}V(t) + \varrho_2\alpha + \rho_2. \end{aligned} \tag{64}$$

By defining $\nu = \left[z^T, \tilde{x}^T, \tilde{\theta}^T, \tilde{\beta}, \tilde{\Theta}^T, \tilde{\Upsilon}_1^T, \ldots, \tilde{\Upsilon}_n^T\right]^T$, and using (41) and Property 1, one has

$$a_1\|\nu\|^2 \leq V(t) \leq a_2\|\nu\|^2, \tag{65}$$

with

$$a_1 = \frac{1}{2}\min\left\{\lambda_{\min}(M(q)), 1, \frac{1}{\lambda_k}, \frac{\lambda_{\min}(K_d)}{\max\limits_{i=1,..,n}(\lambda_{4i})}\right\}, \tag{66}$$

$$a_2 = \frac{1}{2}\max\left\{\lambda_{\max}(M(q)), 1, \frac{1}{\lambda_k}, \frac{\lambda_{\max}(K_d)}{\min\limits_{i=1,..,n}(\lambda_{4i})}\right\}, \tag{67}$$

and $k = 1, 2, 3$. From (63), (65) and theorem 3 in [12], the closed-loop system has a unique global solution, and its state has an asymptotic gain in the second moment. Furthermore, (63) and (65) mean that $V(t) < \infty$, and $\dot{V}(t) < \infty$. Therefore, from the Fubini's theorem [24], we have

$$\int_{t_1}^{t}\mathbb{E}\dot{V}(s)\,ds = \mathbb{E}\int_{t_1}^{t}\dot{V}(s)\,ds = \mathbb{E}V(t) - \mathbb{E}V(t_1), \tag{68}$$

which implies that

$$\mathbb{E}\frac{dV(t)}{dt} = \frac{d\mathbb{E}V(t)}{dt}. \tag{69}$$

Using (69) into (64), multiplying the resulting inequality by $\exp(\rho_3 t)$, and integrating both sides over $[0, t]$, it follows

$$\begin{aligned}\mathbb{E}V(t) \leq & \left(V(0) - \frac{\varrho_2\alpha + \rho_2}{\rho_3}\right)\exp(-\rho_3 t) + \frac{\varrho_2\alpha + \rho_2}{\rho_3} \\ \leq & V(0)\exp(-\rho_3 t) + \frac{\varrho_2\alpha + \rho_2}{\rho_3}. \end{aligned} \tag{70}$$

Taking expectations on both sides of (65), using (70) and the Chebyshev's inequality results in

$$\begin{aligned}\lim_{\rho_4\to\infty}\sup_{t>0}P\{\|\nu(t)\| > \rho_4\} \leq & \lim_{\rho_4\to\infty}\frac{\sup\limits_{t>0}\mathbb{E}\|\nu(t)\|^2}{\rho_4^2} \\ \leq & \lim_{\rho_4\to\infty}\frac{V(0)\exp(-\rho_3 t)}{a_1\rho_4^2} \\ & + \lim_{\rho_4\to\infty}\frac{\varrho_2\alpha + \rho_2}{a_1\rho_3\rho_4^2} \\ = & 0, \end{aligned} \tag{71}$$

which means that $\nu(t)$ is bounded in probability. Therefore, all the closed-loop signals are bounded in probability.

Furthermore, taking expectations on both sides of (41) and using (70) gives

$$\begin{aligned}\lim_{t\to\infty}\mathbb{E}\|\tilde{x}(t)\|^2 \leq & \lim_{t\to\infty}2\mathbb{E}V(t) \\ \leq & \lim_{t\to\infty}\left[2V(0)\exp(-\rho_3 t)\right. \\ & \left. + \frac{2(\varrho_2\alpha + \rho_2)}{\rho_3}\right] \\ \leq & \frac{2(\varrho_2\alpha + \rho_2)}{\rho_3}. \end{aligned} \tag{72}$$

The latter completes the proof □

REFERENCES

[1] A. V. Le, P. Veerajagadheswar, P. T. Kyaw, M. A. Viraj J. Muthugala, M. R. Elara, M. Kuma, and N. H. K. Nhan, "Towards optimal hydro-blasting in reconfigurable climbing system for corroded ship hull cleaning and maintenance," *Expert Syst. Appl.*, vol. 170, May 2021, Art. no. 114519.

[2] V. Prabakaran, A. Vu Le, P. T. Kyaw, R. E. Mohan, P. Kandasamy, T. N. Nguyen, and M. Kannan, "Hornbill: A self-evaluating hydro-blasting reconfigurable robot for ship hull maintenance," *IEEE Access*, vol. 8, pp. 193790–193800, 2020.

[3] M. Fumagalli, R. Naldi, A. Macchelli, F. Forte, A. Q. Keemink, S. Stramigioli, and L. Marconi, "Developing an aerial manipulator prototype: Physical interaction with the environment," *IEEE Robot. Autom. Mag.*, vol. 21, no. 3, pp. 41–50, Sep. 2014.

[4] X. Meng, Y. He, and J. Han, "Survey on aerial manipulator: System, modeling, and control," *Robotica*, vol. 38, no. 7, pp. 1288–1317, Jul. 2020.

[5] M.-Y. Cui, X.-J. Xie, and Z.-J. Wu, "Dynamics modeling and tracking control of robot manipulators in random vibration environment," *IEEE Trans. Autom. Control*, vol. 58, no. 6, pp. 1540–1545, Jun. 2013.

[6] Z.-G. Liu and Y.-Q. Wu, "Modelling and adaptive tracking control for flexible joint robots with random noises," *Int. J. Control*, vol. 87, no. 12, pp. 2499–2510, Jun. 2014.

[7] M. Hui-Fang, D. Na, and Z.-J. Zhang, "Adaptive output-feedback control for stochastic robot system based on neural network," in *Proc. 34th Chin. Control Conf. (CCC)*, Hangzhou, China, Jul. 2015, pp. 1768–1934.

[8] Z. Wu, S. Wang, and M. Cui, "Tracking controller design for random nonlinear benchmark system," *J. Franklin Inst.*, vol. 354, no. 1, pp. 360–371, Jan. 2017.
[9] W. Sun, W. Yuan, J. Zhang, and Q. Sun, "Adaptive tracking control for a class of manipulator systems with state constraints and stochastic disturbances," *Math. Problems Eng.*, vol. 2018, pp. 1–6, Jun. 2018.
[10] W. Sun, S. Diao, S.-F. Su, and Y. Wu, "Adaptive fuzzy tracking for flexible-joint robots with random noises via command filter control," *Inf. Sci.*, vol. 575, pp. 116–132, Oct. 2021.
[11] W. Su, B. Niu, H. Wang, and W. Qi, "Adaptive neural network asymptotic tracking control for a class of stochastic nonlinear systems with unknown control gains and full state constraints," *Int. J. Adapt. Control Signal Process.*, vol. 35, no. 10, pp. 2007–2024, Jul. 2021.
[12] Z. Wu, "Stability criteria of random nonlinear systems and their applications," *IEEE Trans. Autom. Control*, vol. 60, no. 4, pp. 1038–1049, Apr. 2015.
[13] M. Cui and Z. Wu, "Trajectory tracking of flexible joint manipulators actuated by DC-motors under random disturbances," *J. Franklin Inst.*, vol. 356, no. 16, pp. 9330–9343, Nov. 2019.
[14] M. Cui, C. Yang, and Z. Wu, "Global trajectory tracking of a class of manipulators without velocity measurements in random surroundings," *Int. J. Control*, pp. 1–10, Jul. 2021.
[15] H. Wang, W. Ren, C. C. Cheah, Y. Xie, and S. Lyu, "Dynamic modularity approach to adaptive control of robotic systems with closed architecture," *IEEE Trans. Autom. Control*, vol. 65, no. 6, pp. 2760–2767, Jun. 2020.
[16] G. D. Khan, H.-T. Nguyen, and C. C. Cheah, "A stable control strategy for industrial robots with external feedback loop," in *Proc. IEEE Int. Conf. Robot. Autom. (ICRA)*, Xi'an, China, May 2021, pp. 12833–12838.
[17] Z. Liu, B. Chen, and C. Lin, "Adaptive neural backstepping for a class of switched nonlinear system without strict-feedback form," *IEEE Trans. Syst., Man, Cybern., Syst.*, vol. 47, no. 7, pp. 1315–1320, Jul. 2017.
[18] J. J.-B.-M. Ahanda, J. B. Mbede, A. Melingui, and B. E. Zobo, "Robust adaptive command filtered control of a robotic manipulator with uncertain dynamic and joint space constraints," *Robotica*, vol. 36, no. 5, pp. 767–786, May 2018.
[19] M. Krstic and H. Deng, "Stabilization of nonlinear uncertain systems," in *Communications and Control Engineering*, 1st ed. London, U.K.: Springer, 1998.
[20] M.-Y. Cui, Z.-J. Wu, X.-J. Xie, and P. Shi, "Modeling and adaptive tracking for a class of stochastic Lagrangian control systems," *Automatica*, vol. 49, no. 3, pp. 770–779, Mar. 2013.
[21] M.-Y. Cui, Z.-J. Wu, and X.-J. Xie, "Output feedback tracking control of stochastic Lagrangian systems and its application," *Automatica*, vol. 50, no. 5, pp. 1424–1433, May 2014.
[22] R. Datouo, J. J.-B. M. Ahanda, A. Melingui, F. Biya-Motto, and B. E. Zobo, "Adaptive fuzzy finite-time command-filtered backstepping control of flexible-joint robots," *Robotica*, vol. 39, no. 6, pp. 1081–1100, Jun. 2021.
[23] W. He, C. Xue, X. Yu, Z. Li, and C. Yang, "Admittance-based controller design for physical human–robot interaction in the constrained task space," *IEEE Trans. Autom. Sci. Eng.*, vol. 17, no. 4, pp. 1937–1949, Oct. 2020.
[24] F. C. Klebaner, "Introduction to stochastic calculus with applications," in *Plastics*, 3rd ed. Singapore: World Scientific, 2012.

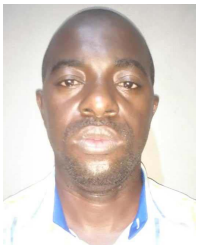

CHARLES MEDZO ABA received the master's degree in electrical engineering from the University of Yaoundé 1, Yaoundé, Cameroon, in 2015, where he is currently pursuing the Ph.D. degree.

His research interests include system modeling, adaptive control, robust control, and robotics.

JOSEPH JEAN BAPTISTE MVOGO AHANDA received the Ph.D. degree in robotics from the University of Yaoundé 1, Yaoundé, Cameroon, in 2019.

He is currently a Senior Lecturer with the Department of Electrical and Power Engineering, The University of Bamenda, Bamenda, Cameroon. His research interests include system modeling, intelligent control, adaptive control, robust control, and robotics.

ACHILLE MELINGUI received the Ph.D. degree in automation and industrial computing from the University of Lille 1, Villeneuve d'Ascq, France, in 2014.

He is currently an Associate Professor with the Department of Electrical and Telecommunications Engineering, Ecole Nationale Supérieure Polytechnique, University of Yaoundé I, Yaoundé, Cameroon. His research interests include modeling and control of mobile robots and continuum manipulators, machine learning, and fuzzy logic.

ROCHDI MERZOUKI received the Ph.D. degree in robotics and automation from the University of Versailles, Versailles, France, in 2002.

He is currently a Professor in control and automation with the Centre de Recherche en Informatique, Signal et Automatique de Lille, UMR, Centre National de la Recherche Scientifique, Polytech Lille, University of Lille, Villeneuve d'Ascq, France. He has authored many contributions published in journals, conference proceedings, and books. His research interests include system of systems, modeling and supervision of mechatronics systems applied to robotics, and intelligent transport.